Scanning Electron Microscopy

Volume 1985
Number 1 *1985*

Article 12

12-7-1984

A Rapid Technique for Counting Cracks in Rocks

W. B. Durham
Lawrence Livermore National Laboratory

J. M. Beiriger
Lawrence Livermore National Laboratory

H. C. Weed
Lawrence Livermore National Laboratory

SCANNING ELECTRON MICROSCOPY/1985/I (Pages 133-142)
SEM Inc., AMF O'Hare (Chicago), IL 60666 USA

0586-5581/85$1.00+.05

A RAPID TECHNIQUE FOR COUNTING CRACKS IN ROCKS

W. B. Durham*, J. M. Beiriger and H. C. Weed

University of California
Lawrence Livermore National Laboratory
Livermore, CA 94550

(Paper received January 19 1984, Completed manuscript received December 7 1984)

Abstract

Using a scanning electron microscope (SEM) and an image analyzer, we have developed a technique for counting and measuring cracks in rocks which is more efficient than traditional techniques in which an operator performs all image analysis functions. The key aspect of the technique is that black-on-white tracings of fresh cracks, which can be made rather rapidly by an operator, are measured and digitized by an image analyzer. The most time-consuming step in the process has now become the generation of SEM micrographs and pertinent chemical (mineralogical) information, not the quantification of crack structure. The technique has been applied to two studies involving nuclear waste isolation in a granitic rock, Climax Stock (Nevada Test Site) quartz monzonite, a Cretaceous age rock which is structurally very inhomogeneous. One study detected a relationship between crack structure and distance from a hammer-drilled borehole; the other study was unable to detect a relationship between crack structure and gamma irradiation treatment in rocks loaded to near failure.

KEY WORDS: crack counting, image analysis, waste isolation, secondary vs backscattered electron imaging, damage in rocks, granites, Climax Stock quartz monzonite

*Address for Correspondence:
W.B. Durham, L-201
U.C.L.L.N.L.
Livermore, CA 94550
Phone Number: 415 - 422-7046

Introduction

Mechanical and transport properties of rocks, such as failure strength, elastic moduli, and fluid permeability, are generally more sensitive to cracks and pores within and between grains of a rock than to the composition of the grains themselves (Walsh and Brace, 1966; Atkinson, 1981). Thus an understanding of important physical processes which manifest themselves as mechanical properties requires characterization of the cracks and pores of a rock. Once characterized and understood, the cracks and pores in a rock serve both for prediction of how the rock will respond to physical change (e.g., how much more load the rock can withstand) and for diagnosis of the change which has already occurred (e.g., how much the rock has been previously loaded).

Microcracks and pores in rocks can be observed and studied in several ways. Indirectly, one can measure cracks and pores through their influence on elastic properties using sonic velocity or elastic strain vs stress as the measured quantities. One can even "hear" microcracks as they form or grow under stress, using acoustic emission techniques. Microstructure can also be observed directly, most commonly by optical microscopy of thin sections and scanning electron microscopy (SEM) of prepared surfaces. Paterson (1978) and Kranz (1983) have reviewed these and other more exotic techniques. Each technique has advantages and drawbacks, with the particular situation generally determining the appropriate technique. In our studies we have used SEM for direct observation because of our need to resolve structural changes on a very fine scale.

During work related to an operating underground nuclear waste storage experiment, called the Spent Fuel Test-Climax or SFT-C (Ramspott et al., 1979), we have undertaken two separate substudies involving use of SEM to characterize the cracks and pores of rock. For both studies, the rock in question was Climax Stock quartz monzonite (CSQM), a granitic rock of Cretaceous age from the site of SFT-C. We discovered quickly that CSQM is structurally a highly heterogeneous rock and that in order to

use the predictive/diagnostic ability the cracks provide, we would have had to observe and measure hundreds of cracks. Resources for the substudies were rather limited, so rather than make detailed, individual measurements of cracks manually (e.g., Sprunt and Brace, 1974; Hadley, 1976; Tapponnier and Brace, 1976; Kranz, 1979, 1980; Spetzler et al., 1981; and Chernis, 1983) we attempted to increase measurement speed through simplification and partial automation.

The Two Studies

The experimental nuclear waste repository, SFT-C, is located approximately 420 m below ground level in the Climax Stock, in the NE corner of the Nevada Test Site. Eleven spent fuel assemblies sealed in stainless steel canisters were stored in an array of other (electrical) heat sources in order to simulate, in the central region of the array, the conditions within a very large repository. Our substudies were (1) Study A, an assessment of damage to rock incurred during hammer drilling of the canister emplacement holes (i.e., the holes into which fuel assembly canisters were placed), and (2) Study B, a study of the failure mechanism in CSQM as a function of gamma-ray dosage to the rock. In particular, we were interested in finding out if crack growth prior to failure in CSQM was influenced by prior gamma irradiation. Both studies were aimed at confirming that the structural integrity of the experimental repository was not compromised by normal repository operations and conditions. In both studies, the SEM sections were 25.4 mm diameter cores, prepared by the method outlined below. For Study A, the cores were taken directly from the wall of the canister emplacement hole (Figure 1). For Study B, cores 25.4 mm in diameter by 63 mm long were taken to the laboratory and half of them given a gamma ray dosage of approximately 10 MGy (10^9 rads) from a ^{60}Co source. The other half were used as control samples. All were then end-loaded to near failure and then cut through their circular midplane to provide the SEM sections. Microcracks induced by the compressive load tend to run parallel to the load (i.e., the cylinder) axis. Hence the SEM section was taken normal to the major crack direction in order to intersect as many cracks as possible.

Further details on Study A are given in Weed and Durham (1982) and on Study B in Beiriger and Durham (1984).

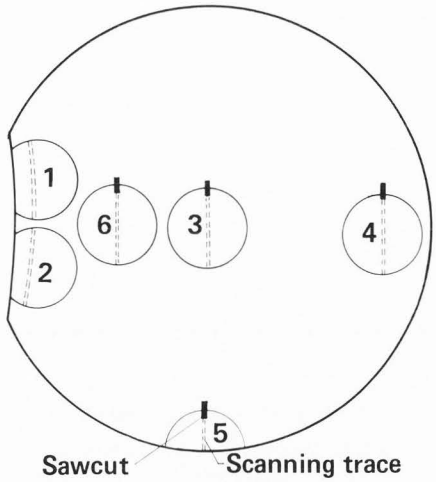

Fig. 1. The location of six 25.4 mm diameter sections (numbered 1-6) used in Study A with respect to the canister emplacement hole. The viewing direction is parallel to the axis of the canister emplacement hole. Heavy marks across the circumferences of the 25.4 mm diameter sections are orienting saw cuts. Dashed lines indicate the positions of the SEM traces.

Techniques

Sample Preparation and SEM Operation

Sections were cut on a diamond saw to a thickness of 5 mm, and approximately 1 mm was rough ground from the face of interest in order to remove cutting damage. They were then polished with abrasive grit and finished with 2 μm alumina on a cloth lap. The polished surfaces were next ion-milled in order to remove the thin layer (10-20 μm) which had been smeared and damaged by the polishing procedure. After ion milling, samples were coated with approximately 20 nm of carbon by vacuum evaporation to increase surface conductivity and prevent static charge accumulation under electron bombardment in the SEM. This method generally follows that outlined by Brace et al. (1972) and is probably the most commonly used preparation technique for the SEM study of rocks.

The SEM used was an AMR (AMRAY) 1000 equipped with a Kevex 7000 energy dispersive spectrometer (EDS). In all cases, the working distance was 12 mm and the accelerating voltage was 20 kV. For some of the work the secondary electron (SE) detector was used to generate micrographs and in other cases a quadrupole solid-state backscattered electron (BSE) detector was used. When the SE detector was used, the specimen tilt angle was set at 30° and a slightly positive potential was applied to the cage over the scintillator in order to increase the proportion of BSE relative to SE. We found that at intermediate magnification ranges microfractures stand out in better contrast when the proportion of BSE is higher, no doubt because of the sharp change in topography which an open microfracture defines. With the quadrupole BSE detector, specimen tilt angle was set to 0° (the detector was positioned on the pole piece of the electron column). Interestingly, the topographic contrast provided by microcracks in this mode was not as strong as the chemical contrast they provided (since cracks have zero atomic weight), so the polarity of the poles of

the detector was set to maximize chemical differences. The mode using the SE detector is hereafter referred to as the BSE/SE mode and that using the BSE detector as the BSE mode.

Microcrack Measurement

All micrographs used for measurement purposes covered approximately 0.035 mm^2 of rock (500X magnification). In order to minimize operator bias toward "interesting" areas, the photographic conditions and locations (referred to as "spots") to be photographed were selected before specimens were introduced into the SEM. Figure 1 shows the selection for Study A. In both studies, micrographs were taken at 2 mm intervals (as determined by vernier settings of the stage controls) along a linear trace across the section. The orientation of the trace was arbitrary, but again, preselected. The trace was either a diameter or within 2 mm of the diameter of the section. Starting and ending points were allowed no closer than 1 mm to the edge of the section in order to avoid possible artifacts of coring. Thus a given trace yielded seven to nine micrographs upon which measurements could be made. Additionally, a low magnification overview was made every second or third spot for mapping purposes to cover the eventuality that some spots would have to be reinvestigated.

At every spot, a qualitative chemical analysis of every grain was made with the EDS. Ninety-nine percent of the volume of CSQM is made up of one of five different mineral phases, so qualitative analysis was adequate for mineral identification. Although we did not know it at the time the SEM work was being done, the chemical information turned out not to be used in any of the post-measurement analysis.

The crack quantification procedure consisted of three steps: (1) operator discrimination of fresh cracks; (2) digitization of the discriminated crack pattern; and (3) numerical analysis of the digitized image.

The first step required some subjective operator decisions to discriminate pre-existing cracks from "fresh" cracks introduced by operations associated with SFT-C (in the case of Study A) or by laboratory testing (Study B). A crack was usually judged on the basis of physical appearance: a sharply defined edge and pieces which fit together marked an obvious fresh crack; a crack which intersected many pores and had a varying width along its trace or which was partially filled with material fixed to the crack walls was obviously pre-existing. Figure 2 shows examples of fresh and pre-existing cracks. A full spectrum of cracks existed, grading from obviously fresh to obviously pre-existing, so operator judgments were sometimes arbitrary. We tried to shield the data from being systematically affected by day-to-day variations in the quality of operator judgment. In particular, when the judgments were made (by tracing, see below), the identity of the micrographs was masked and the order of measurement was randomized by shuffling the micrographs.

Digitization, step (2), was accomplished by making pencil tracings of the fresh cracks on transparent, matte-finish overlays, one micrograph at a time, then photocopying the overlays on white paper to produce an unambiguous black on white image of the cracks. Figures 2 and 3 illustrate the results of the process for the BSE and BSE/SE modes of operation. The photocopied image was then digitized and analyzed with a Quantimet 720 image analyzer, which converted the image into a list of cracks along with their areas, perimeters, and locations. Since all cracks had been forced to have the same width (the width of a pencil trace), the area and perimeter information were combined to give a single parameter which we call the crack length, the length of the line formed by the intersection of the crack plane and the exposed rock surface. By an operator-invoked convention within the image analyzer, two intersecting cracks were counted as two cracks.

Numerical analysis, step (3), was a matter of transferring the image analyzer lists to a larger computer, combining the lists into one large table, and deriving the desired information from the large table using database analysis software.

In summary, by simplifying crack measurement to a single parameter (length), and using an image analyzer in a fairly unsophisticated mode, we were able to greatly reduce the operator time involved in measurement. The key step, identification and tracing of fresh cracks, required well under one minute per micrograph. Processing in the image analyzer (including setup) averaged 2-3 minutes per micrograph. In the two studies, the average number of cracks per micrograph was 5.6; hence, the total time spent quantifying microfractures was well under one minute per crack. In fact, operating the SEM and EDS became the longest step of the process, requiring roughly 15 minutes per spot, or 3 minutes per fresh crack.

Results

In Study A, two traces were run on each of six sections (orientation with respect to the canister emplacement hole is shown in Figure 1), resulting in 88 spots photographed and 674 fresh cracks identified and measured. All micrographs were taken in BSE/SE mode. In Study B three traces were run on each of nine sections, resulting in 207 spots and 990 fresh cracks. One of the three traces on each section was run in BSE/SE mode, the other two in BSE mode.

From the measurements, we computed three parameters (only two of which are independent): crack density (number of cracks per unit area), average crack length, and average length of crack per unit area. In Study A, all measurements on a given section were combined to give a single set of parameters. A plot of any given parameter vs

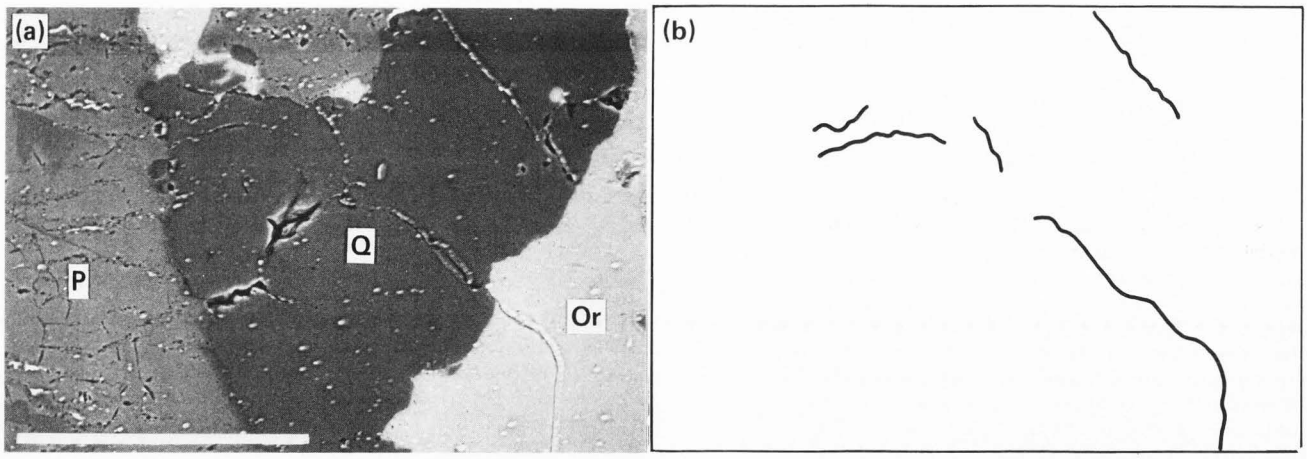

Fig. 2. Crack counting example, BSE pass. (a) SEM photomicrograph, scale bar = 100 μm; (b) cracks identified as fresh, same magnification as (a). There are five fresh cracks identified here ranging in length from 19 to 113 μm with mean length 48.0 μm. The three major phases are, in order of increasing brightness, quartz ("Q"), plagioclase ("P"), and orthoclase ("Or"). The subtle shadings in the plagioclase probably represent local variations of the Ca/Na ratio within a single grain. The small bright grain at the top was not identified. The many other crack-like features, most of which are in the plagioclase grain, were judged to be pre-existing on the basis of the criteria discussed in the text.

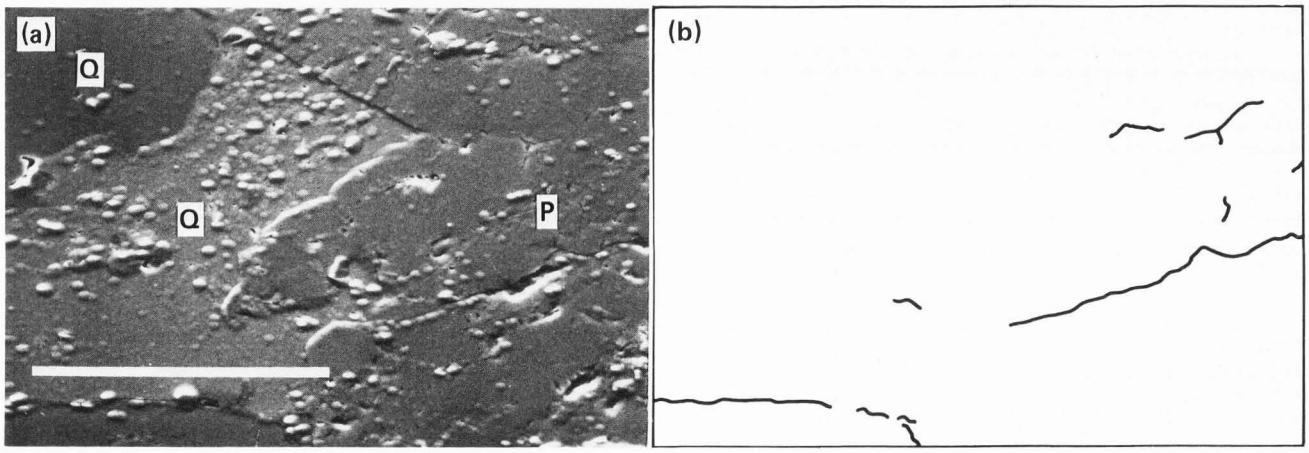

Fig. 3. Crack counting example, BSE/SE pass. (a) SEM photomicrograph, scale bar = 100 μm; (b) cracks identified as fresh, same magnification as (a). There are ten fresh cracks identified here ranging in length from 4 to 104 μm. Mean length is 24.5 μm. Most of the right half of the picture area is a plagioclase grain (labeled "P"). A single quartz grain ("Q") dominates most of the left half of the picture (lighter contrast). Two other quartz grains are at the upper left and lower right. Note the poorer grain-to-grain contrast as compared to Fig. 2.

section, appropriately adjusted for the distance between the center of the section and the wall of the emplacement hole, gave a measure of crack damage as a function of distance from the hole (Figures 4 and 5). Figures 4 and 5 show that material within the first few tens of millimeters of the canister emplacement hole is more cracked than material further out. The figures also show that a great deal of scatter exists in the data. In trace-to-trace comparisons of density or average length in any given section, differences of a factor of two are not unusual.

The scatter in the data became a serious problem in Study B. The three crack parameters are compiled by trace and by sample in Table 1 in order to illustrate the scatter. Again,

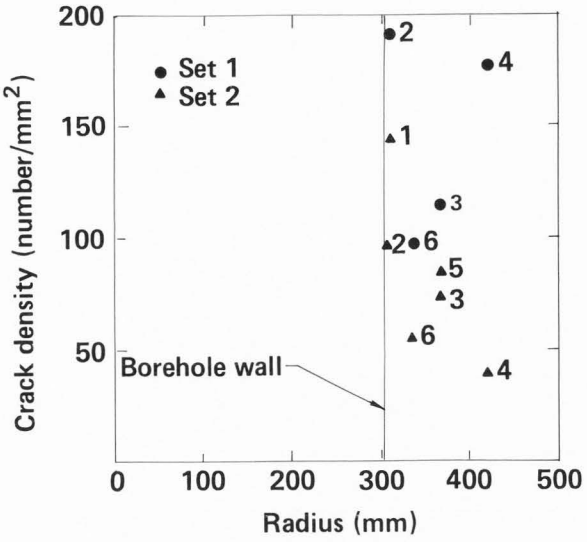

Fig. 4. Crack density vs distance from the center of the canister emplacement hole for Study A. Numbers next to each of the symbols correspond to section locations in Figure 1. Triangles indicate the results for one trace on each section; circles, that for the other trace. For sections 1 and 5, the trace statistics are combined.

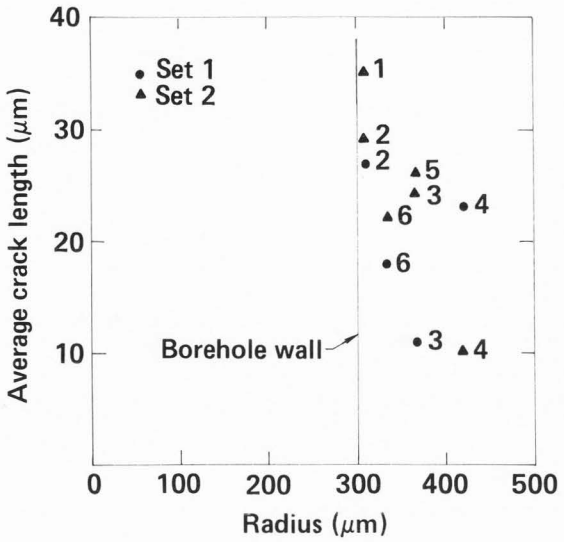

Fig. 5. Average crack length vs distance from the center of the canister emplacement hole for Study A. Same conventions apply as for Figure 4.

note that differences of a factor of two are not unusual, even when the BSE traces alone are compared. The scatter is so large that when the crack parameters are grouped by radiation treatment (Table 2), they are only subtly different and are accompanied by standard deviations which are comparable to the means. Hence, we were not able to resolve a dependence on radiation treatment.

Note that in Tables 1 and 2 the BSE/SE mode in the SEM appears to reveal more cracks than the BSE mode. The cracks so revealed in BSE/SE, however, are on average less than half as long as those revealed in BSE, resulting in an average total length of crack per unit area that is slightly greater in BSE. Comparisons of the two techniques on the same area of rock indicate the probable cause of the difference in crack statistics is the sharper contrast (and perhaps better resolution) provided by the BSE mode: a long crack seen in BSE is occasionally mistaken for two or more shorter cracks in BSE/SE. The net result is a higher number density in BSE/SE but a higher length density in BSE, consistent with Tables 1 and 2.

Discussion and Conclusions

Is it possible that the technique itself is responsible for the large scatter in the data? There is good evidence against this, based on a comparison of CSQM and other granites.

Among granitic rocks which have been mechanically tested and otherwise observed in the laboratory, CSQM is unusually heterogeneous. (Note that this is not because CSQM is an unusual rock; laboratory testing materials are frequently selected on the basis of homogeneity.) Petrographically, CSQM is strongly heterogeneous on the millimeter scale (Fig. 6). Most of the rock is composed of grain sizes ranging from 0.25 to 2 mm, but contains irregular quartz phenocrysts (about 10% by volume) typically 5 mm across and potassium feldspar phenocrysts (about 5% by volume) that are as much as 150 mm long. In contrast Westerly granite is finer-grained (0.25 to 1 mm) and petrographically much more uniform than CSQM. Comparison of failure strength statistics for CSQM and other granites is striking: for Westerly, one standard deviation is <3% of the mean at 100 MPa confining pressure (Costantino, 1978). Kranz and Scholz (1977) indicate that the unconfined strength of Barre granite is 220 ± 10 MPa (although they give no raw data). The scatter in unconfined strength of Oshima granite is clearly less than ±5% based on eight test results published by Sano et al. (1981). For CSQM unconfined, one standard deviation is typically >15% of the mean.

The trend toward lower scatter in the more homogeneous granites carries over to quantitative crack measurement. Crack statistics on Westerly and Barre granites based on manual techniques are compared to our measurements in Table 3. Each of the four other studies in Table 3 has precise enough statistics to indicate that either the number of cracks or the length of cracks, or both, increases with magnitude and duration of load.

To put matters in perspective, the motivation for speeding up the crack counting procedure resulted from dealing with an inhomogeneous material. The semi-automated procedure was developed during the course of Study A when it became apparent that

TABLE 1: Crack Statistics by Sample, Study B.

Sample		No. of cracks counted	Areal number density (mm^{-2})	Average length (μm)	Areal length density (mm/mm^2)
2 (no γ[a])	b	18	85	52	4.41
		31	177	14	2.47
		38	120	30	3.59
3 (γ)		45	157	30	4.70
		66	206	14	2.79
		20	81	32	2.64
4 (no γ)		23	109	36	3.98
		48	171	15	2.54
		51	182	26	4.67
5 (γ)		22	90	41	3.66
		49	124	14	1.74
		22	75	33	2.46
6 (no γ)		12	57	35	1.99
		64	214	12	2.47
		15	71	44	3.12
7 (γ)		25	119	36	4.27
		62	158	13	2.07
		30	107	38	4.01
8 (no γ)		49	175	28	4.89
		45	117	15	1.78
		14	67	29	1.95
9 (γ)		24	114	34	3.88
		46	131	16	2.15
		47	167	23	3.78
10 (no γ)		18	86	30	2.53
		71	285	16	4.44
		35	125	33	4.06

[a] γ = gamma irradiation.

[b] Each of the groups of three numbers gives the statistics for { BSE pass 1 / BSE/SE pass. / BSE pass 2

Fig. 6. Low magnification SEM photomicrograph illustrating the heterogeneity of grain sizes in CSQM. Section is taken from the group of control samples of Study B (see text). Image is BSE only and the scale bar represents 1 mm. The four major contrast levels indicate, in order of increasing brightness, quartz ("Q"), plagioclase ("P"), orthoclase ("Or"), and biotite ("B"). Small bright spots are various heavier element phases such as iron oxide and zircon. Not shown is the variation in grain size of orthoclase: phenocrysts 100 mm across are not unusual. The grain scale heterogeneity of CSQM may be the principal cause of the noisy crack and strength measurements made on this rock.

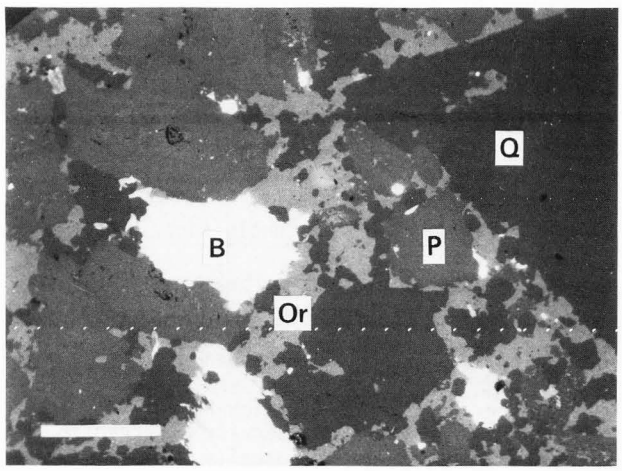

TABLE 3: Comparison of Crack Counting Studies using SEM.

Studies	Rock	Loading conditions	Confining pressure (MPa)	No. counted	Density (mm^{-2})	$\bar{L}$ (μm)	$\overline{L/area}$ (mm/mm^2)
Sprunt and Brace (1974)	Westerly granite	Virgin	--	80		3-10[a]	
		0.95σ_f[b]	Not given	80	10-30[a]		
Hadley (1976)	Westerly granite	Virgin	--	344[c]		1-5[a]	
	" " (T5)	>0.95σ_f	50	632[c]		10-50[a]	
	" " (W5)	Failed	150	850[c]		10-50[a]	
Tapponnier and Brace (1976)	Westerly granite	Virgin	--	182[d]	196 ± 73[e]		
	" " (T3)	0.58σ_f	50	502[d]	239 ± 48[e]		
	" " (T5)	>0.95σ_f	50	861[d]	354 ± 102[e]		
Kranz (1979)	Barre granite	Virgin	--	56	7[f]	54 ± 36	
	" "	0.87σ_f, 7s	0.1	262	26[f]	72 ± 42	
	" "	" , 37s	"	282	23[f]	90 ± 79	
	" "	" ,125s	"	190	9[f]	146 ± 91	
	" "	" ,136s	"	183	8[f]	164 ± 88	
This study[g]	CSQM	Virgin	--	54	91 ± 91[h]	36 ± 47	3.24 ± 3.16
	" , no γ	0.80±.24σ_f	0.1	235	115 ± 105	32 ± 30	3.64 ± 3.42
	" , γ	0.93±.21σ_f	0.1	273	113 ± 100	32 ± 33	3.61 ± 3.15
Kranz (1980)	Barre granite	0.87σ_f[i]	0.1	172	7[f]	172 ± 181	
	" "	"	53	246	15[f]	230 ± 282	
	" "	"	100	254	15[f]	245 ± 302	
Spetzler et al. (1981)	Pyrophyllite	Virgin	0.1	Not given		<40	
	" "	Virgin	30	Not given		<40	
	" "	Failed	5	91	--	80[j]	
	" "	Failed	30	123	--	80[j]	

TABLE 2: Crack Statistics by Irradiation Treatment, Study B.

	No. counted	Density (mm^{-2})	$\bar{L}$[a] (μm)	$\overline{L/area}$ (mm/mm^2)
BSE/SE Trace				
No γ[b]	223	149 ± 153[c]	14 ± 12	2.11 ± 2.31
γ	259	190 ± 178	14 ± 13	2.71 ± 2.64
BSE Traces				
No γ	235	115 ± 105	32 ± 30	3.64 ± 3.42
γ	273	113 ± 100	32 ± 33	3.61 ± 3.15
Untreated, unstressed	54	91 ± 91	36 ± 47	3.24 ± 3.16

[a] $\bar{L}$ = average crack length.

[b] γ = gamma irradiation.

[c] One standard deviation, assuming normal distribution.

[a] Median values.

[b] σ_f = failure strength.

[c] Includes pores.

[d] Cracks encountered in axial traverses not included.

[e] Approximated as

$$\text{density} = \frac{\text{No. of crack intersections along traverse}}{\text{Traverse length}} \times \frac{\text{Traverse length}}{mm^2} .$$

[f] Approximated as

$$\text{density} = \frac{\text{No. intersections}}{\text{Trace length}} \times \frac{1}{\bar{L}} .$$

[g] BSE data only; Sample 2 (which failed) not included.

[h] One standard deviation.

[i] At the onset of tertiary creep.

[j] Cracks shorter than 50 μm not included.

qualitative SEM examination would not produce useful results and that manual measurement would quickly use up the resources allocated to the study. As it turned out, CSQM was so heterogeneous that even the semi-automated technique was barely acceptable: Study A gave a useful result (hammer drilling damage is confined to a 10-30 mm skin around the borehole) but Study B did not (gamma irradiation may or may not enhance microfracturing under load prior to failure).

Analysis of the time spent on the various aspects of our semi-automated crack quantization technique indicates that roughly 10-20% of operator time is spent identifying fresh cracks and tracing SEM images, roughly 30% of the time is spent processing line images in the image analyzer, and 50% of the time is spent generating SEM micrographs and chemical information pertaining to minerals present in the micrographs. It is interesting to note that further speed increase can be accomplished with relatively unsophisticated, presently available (but perhaps expensive) items: automatic sample feeding, stage stepping, focusing, and microphotography for the SEM; and automatic feeding for the image analyzer. The most difficult task in total automation, machine discrimination of fresh cracks, would only slightly speed up our present procedure. Such artificial intelligence would, however, greatly improve the quality of measurement by eliminating operator bias and by providing information on such important parameters as crack width, straightness, and interconnectivity.

Acknowledgments

We thank Gene Simmons, Paul Tapponnier, and Modesto Montoto for critically reviewing the manuscript. Work performed under the auspices of the U.S. Department of Energy by the Lawrence Livermore National Laboratory under contract number W-7405-ENG-48. This study was conducted as part of the Nevada Nuclear Waste Storage Investigation of the U.S. Department of Energy.

References

Atkinson B. (1981). Cracks in rocks under stress. Nature 290, 632.

Beiriger JM, Durham WB. (1984). SEM studies of stressed and irradiated Climax Stock quartz monzonite. University of California, Lawrence Livermore National Laboratory Report UCID-20052, 23 pp.

Brace WF, Silver E, Hadley K, Goetze C. (1972). Cracks and pores: A closer look. Science 178, 162-164.

Chernis PJ. (1983). Notes on the pore-microfracture structure of some granitic samples from the Whiteshell Nuclear Research Establishment, Technical Record TR-226. Atomic Energy of Canada Limited, Pinawa, Manitoba, 34 pp.

Costantino MS. (1978). Statistical variation in stress-volumetric strain behavior of Westerly granite. Int. J. Rock Mech. Min. Sci. 15, 105-111.

Hadley K. (1976). Comparison of calculated and observed crack densities and seismic velocities in Westerly granite. J. Geophys. Res. 81, 3484-3494.

Kranz RL. (1979). Crack growth and development during creep of Barre granite. Int. J. Rock Mech. Min. Sci. 16, 23-25.

Kranz RL. (1980). The effects of confining pressure and stress difference on static fatigue of granite. J. Geophys. Res. 85, 1854-1866.

Kranz RL. (1983). Microcracks in rocks: A review. Tectonophys. 100, 449-480.

Kranz RL, Scholz CH. (1977). Critical dilatant volume of rocks at the onset of tertiary creep. J. Geophys. Res. 82, 4893-4898.

Paterson MS. (1978). Experimental Rock Deformation - The Brittle Field. Springer-Verlag, New York, pp. 120-135, 147-157.

Ramspott LD, Ballou LB, Carlson RC, Montan DN, Butkovich TR, Duncan JE, Patrick WC, Wilder DG, Brough WT, Mayr MC. (1979). Technical concept for a test of geologic storage of spent reactor fuel in the Climax granite at the Nevada Test Site. University of California, Lawrence Livermore National Laboratory Report UCRL-52796, 47 pp.

Sano O, Ito I, Terada M. (1981). Influence of strain rate on dilatancy and strength of Oshima granite under uniaxial compression. J. Geophys. Res. 86, 9299-9311.

Spetzler HA, Sobolev GA, Sondergeld CH, Salov BG, Getting IC, Koltsov A. (1981). Surface deformation, crack formation and acoustic velocity changes in pyrophyllite under polyaxial loading. J. Geophys. Res. 86, 1070-1080.

Sprunt ES, Brace WF. (1974). Direct observation of microcavities in crystalline rocks. Int. J. Rock Mech. Min. Sci. 11, 139-150.

Tapponnier P, Brace WF. (1976). Development of stress-induced microcracks in Westerly granite. Int. J. Rock Mech. Min. Sci. 13, 103-112.

Walsh JB, Brace WF. (1966). Elasticity of rock: A review of some recent theoretical studies. Felsmechanik und Ingenieurgeologie 4, 283-297.

Weed HC, Durham WB. (1982). Drilling-induced borehole-wall damage at Spent Fuel Test-Climax. University of California, Lawrence Livermore National Laboratory Report UCID-19672, 23 pp.

Discussion with Reviewers

M. Montoto: Before the specimen preparation, did you try any kind of bulk or superficial impregnation, with a penetrant whose Z value would contrast with those of the rock-forming minerals of your rocks, for an easier discrimination of the thus impregnated open spaces under the BSE mode?
Authors: No. Penetrants help identify only the so-called "connected porosity" in a rock. The kind of damage we were attempting to identify surely included significant numbers of isolated microcracks and we had no desire to exclude such cracks from our measurements. Furthermore, penetrants do not distinguish fresh from pre-existing cracks in the connected crack network, so would raise the background "noise" level of crack measurements.

M. Montoto: I have been concerned with a similar problem to yours ("Rockstore '80, Subsurface Space", M. Bergman, Ed., vol. 3, pp. 1357-1368, Pergamon Press, 1981), and I tried to solve it also through image analysis procedures. I agree that a semi-automatic procedure is the only viable method to quantify rock-forming components (cracks, pores, minerals, texture, . . .). We use fluorescein-dye-impregnated, polished and metallized thin sections, which are studied by means of different optic and electronic microscope techniques in order to map the above mentioned components. Have you tried out anything for mapping purposes and further quantification?
Authors: We have had limited success with photographic mapping of fluorescein-dye-impregnated macrocracks (lengths >0.5 mm). However, when our preliminary studies of CSQM indicated that, like other granites, there was an important population of cracks with lengths of order 10 μm, we abandoned the optical techniques. A few years ago, we pursued crack decoration with cathodoluminescent salts, in order to use the high resolving power of the SEM, but we never managed to stumble upon a cathodoluminescent material with sufficient brightness and longevity under the electron beam to decorate the cracks we were interested in.

Reviewer III: Why was it necessary to use the SEM for fracture detection rather than a light microscope? Could not the measurements have been made easier by using a light-pen type digitizing tablet? This would have accomplished crack tracing and length measurement in one step.
Authors: We needed the high resolving power of the SEM to identify many of the smaller microcracks. Consider, for example, the small "pre-existing" fractures in the plagioclase grain in Figure 2. They would barely be resolved optically, and surely would be mistaken for "fresh" cracks.

A light pen and digitizing tablet probably would work well in this application and also would save a little time. We used the Quantimet 720 simply because it was immediately available and a digitizing tablet was not.

Reviewer III: Were all microphotos taken at the same magnification? The degree of magnification will seriously affect the number of cracks detected. Was the used magnification appropriate or would additional cracks be detected at higher magnification?
Authors: All microphotos used for crack counting were taken at 500X. This selection of magnification was not arbitrary. The resolution limit of the SEM in the BSE and BSE/SE mode we employed was approximately 0.1 μm (this varies with accelerating voltage and spot size, of course). The intrinsic photographic resolution at 500X is also about 0.1 μm, so we selected that magnification in order to include as much surface area as possible without losing sight of any microcracks. Thus the answer to the second question is that no additional cracks would be detected at higher magnification. Note that switching to SE mode improves our resolution by an order of magnitude, but in SE mode cracks stand out in dramatically poorer contrast, for reasons discussed in the text. Had we pursued the study at 5000X in SE, we probably would have measured a higher crack number density, but it would have required 100 times as many micrographs to cover the same area, and cracks longer than about 20 μm would have been truncated by the edges of the micrographs. Had we pursued the study at 500X in SE, we would have identified a lower number of cracks per unit area.

Reviewer III: Were all cracks observed and measured by the same operator or were several people involved?
Authors: You correctly perceive that operator bias, both in the image-making and in crack discrimination is a critical factor to be reckoned with. All crack discrimination in Study A was done by one person (WBD) and in Study B by one person (JMB). SEM work in Study A set 1 was done by one person (WBD), Study A set 2 by one person (HCW), and Study B by one person (JMB). Day-to-day variations in mental attitude and machine performance are assumed to be folded in with the noise. In any of the discussions of results, no cross comparisons (save disinterested psychological conjectures) were made of Study A and Study B, or of Study A set 1 and Study A set 2.

Reviewer III: One might expect drilling-induced cracks to have a preferred orientation, different from naturally occurring cracks. Was this the case?
Authors: For drilling-induced cracks (Study A), this may well be true, although preferred orientation may be more pronounced in some subset of fresh cracks (e.g., the longer ones). In any case, we did not attempt to find a preferred orientation because (a) it was not qualitatively obvious, and (b) the low signal-to-noise ratio of the crack statistics was

discouraging (although we note that identification of a preferred orientation might serve to improve the signal-to-noise ratio).

For cracks introduced by uniaxial compression (Study B), it is now well established that a strong preferred orientation develops: crack plane normals lie in the "horizontal" plane, normal to the direction of applied load (see, for instance Tapponnier and Brace, 1976). There is no preferred orientation of crack normals in the horizontal plane.